ACS Medicinal Chemistry Letters

Letter

The Antitumor Potential of the Isoflavonoids (+)- and (–)-2,3,9-Trimethoxypterocarpan: Mechanism-of-Action Studies

Kaio Farias, Roner F. da Costa, Assuero S Meira, Jairo Diniz-Filho, Eveline M. Bezerra, Valder N. Freire, Prue Guest, Maryam Nikahd, Xinghua Ma, Michael G. Gardiner, Martin G Banwell, Maria da C. F. de Oliveira, Manoel O. de Moraes, and Claudia do Ó. Pessoa

ACS Med. Chem. Lett., **Just Accepted Manuscript** • DOI: 10.1021/acsmedchemlett.0c00097 • Publication Date (Web): 20 May 2020

Just Accepted

is published by the American Chemical Society. 1155 Sixteenth Street N.W., Washington, DC 20036

The Antitumor Potential of the Isoflavonoids (+)- and (–)-2,3,9-Trimethoxypterocarpan: Mechanism-of-Action Studies

Kaio Farias,[a] Roner F. da Costa,[b] Assuero S. Meira,[a] Jairo Diniz-Filho,[a] Eveline M. Bezerra,[b] Valder N. Freire,[c] Prue Guest,[d] Maryam Nikahd,[d] Xinghua Ma,[d] Michael G. Gardiner,[d] Martin G. Banwell,[d,e,*] Maria da C. F. de Oliveira,[f] Manoel O. de Moraes,[a] and Claudia do Ó. Pessoa[a,*]

[a] Department of Physiology and Pharmacology, Faculty of Medicine, Federal University of Ceará, Fortaleza, CE, 60430-275, Brazil.

[b] Department of Natural Sciences, Mathematics and Statistics, Federal Rural University of the Semi-Arid Region - UFERSA, Mossoró - RN, Brazil.

[c] Department of Physics, Science Center, Federal University of Ceará, Fortaleza, CE, 60430-275, Brazil.

[d] Research School of Chemistry, Institute of Advanced Studies, The Australian National University, Canberra, ACT 2601, Australia.

[e] Institute for Advanced and Applied Chemical Synthesis, Jinan University, Guangzhou, 510632, China.

[f] Department of Organic and Inorganic Chemistry, Science Center, Federal University of Ceará, Fortaleza, CE, 60430-275, Brazil.

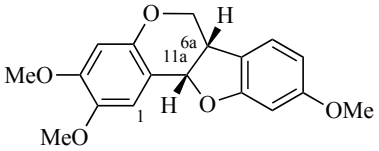

(+)-**1**

a pterocarpan first encountered in the Brazilian tree *Platymiscium floribundum* Vogel. (Fabaceae) and prepared by synthesis for this study

IC_{50} µg/mL

HL-60: 0.06 (0.02*)
HCT-116: 0.73
OVCAR-8: 0.54 (0.34*)
SF-295: 1.09 (0.04*)
*corresponding values for doxorubicin
(–)-**1** much less active

ABSTRACT: Synthetically-derived samples of (+)-(6a*S*,11a*S*)-2,3,9-trimethoxypterocarpan [(+)-**1**] and its enantiomer [(–)-**1**], both of which are examples of naturally-occurring isoflavonoids, were evaluated, together with the corresponding racemate, as cytotoxic agents against the HL-60, HCT-116, OVCAR-8 and SF-295 tumor cell lines. As a result it was established that compound (+)-**1** was particularly active with OVCAR-8 cells being the most sensitive and responding in a dose-dependent manner. A study of cell viability and drug-induced morphological changes revealed the compound causes cells death through a mechanism characteristic of apoptosis. Finally, a computational study of the interactions of compound (+)-**1** and (*S*)-monastrol, an established, synthetically-derived, potent and cell-permeant inhibitor of mitosis, with the kinesin-type protein Eg5 revealed that both bind to this receptor in a similar manner. Significantly, compound (+)-**1** binds with greater affinity, an effect attributed to the presence of the associated methoxy groups.

KEYWORDS: anticancer agents, Eg5, molecular docking, OVCAR-8 cell-line, pterocarpan

During the course of screening natural products as potential anti-cancer agents,[1,2] the pterocarpans[3] have become recognized for their diversity of biological activities that span anti-inflammatory, anti-microbial, anti-malarial, anti-estrogenic, anti-diabetic as well as anti-tumor effects. These isoflavonoids are characterized by the presence of mutually annulated benzofuran and benzopyran rings and so creating the parent and *cis*-fused 6a,11a-dihydro-6*H*-benzofuro[3,2-*c*]chromene (tetracyclic) ring-system that embodies stereogenic centres at C6a and C11a and that are more commonly both *R*-configured in the naturally-occurring compounds.[2] One member of this family, and the subject of previous studies by some of us,[4-7] is (+)-(6a*S*,11a*S*)-trimethoxypterocarpan [(+)-**1**, Figure 1], a compound isolated from the heartwood of the Brazilian tree *Platymiscium floribundum* Vogel. (Fabaceae) and shown to exert high cytotoxicities (IC_{50} 0.1-2.9 μg/mL) against leukemia (HL-60 and CEM), breast (MCF-7), colon (HCT-8), and skin (B16) cancer cell-lines.[4] Furthermore, in an antimitotic assay using sea urchin eggs, pterocarpan (+)-**1** showed log IC_{50} values of –8.10 M (1st cleavage), –7.91 M (2nd cleavage) and –7.97 M (blastulation).[5]

The high cytotoxicity of compound (+)-**1** against the leukemia cell line HL-60 (IC_{50} 0.1 μg/mL),[4] prompted us to begin investigating its mode of action[6] and so revealing this involves both inhibition of DNA synthesis and the triggering of apoptosis, the latter arising through mitochondrial depolarization and caspase-3 activation. Parallel studies established that the anti-proliferative effects of compound (+)-**1** extended beyond HL-60 to other human leukemia cell lines (*viz*. K562, Jurkat and Molt-4) and its high selectivity towards these was revealed when tested against (healthy) human peripheral blood mononuclear cells (PBMCs).[7] So after challenging the PBMCs with the natural product (administered at 10 μg/mL) for 72 h 81% of them remained viable.

Figure 1. The structure of (+)-(6a*S*,11a*S*)-2,3,9-trimethoxypterocarpan [(+)-**1**] [isolated from *Platymiscium floribundum* Vogel. (Fabaceae)] and its enantiomer (–)-**1** [isolated from *Pisum sativum* Linn. (Fabaceae) infected with *Fusarium solani*]

While all of the above-mentioned studies were performed using the naturally-derived and 6a*S*,11a*S*-configured compound (+)-**1**, it should be noted that its enantiomer, *viz*. (–)-(6a*R*,11a*R*)-2,3,9-trimethoxypterocarpan or (–)-**1** (Figure 1), has been isolated from *Pisum sativum* Linn. (Fabaceae) infected with *Fusarium solani*.[8]

In order to more fully understand the structural features within compound (+)-**1** that underpin its potent and selective cytotoxic effects, we now report on the analogous studies of its enantiomer and the corresponding racemate. These compounds, together with the original one [*viz*. (+)-**1**] were obtained by total synthesis and their activities evaluated against HL-60 (promyelocytic leukemia), HCT-116 (colon), OVCAR-8 (ovarian adenocarcinoma) and SF-295 (glyoblastoma) tumor cell-lines. In addition, we detail the outcomes of *in silico* docking studies conducted in order to evaluate the interaction of (+)-2,3,9-trimethoxypterocarpan [(+)-**1**] with the kinesin-type protein Eg5. This particular aspect of the present study was motivated by our earlier observations[9] that compound (+)-**1** causes an increase in the number of mitotic cells incorporating monoastral spindles surrounded by condensed chromosomes.[10] In addition, by using an immunofluorescence staining assay involving an anti-γ-tubulin antibody, it was revealed that the (+)-form of the natural product blocks centrosome segregation. Such properties resemble those reported for monastrol (MON),[11] a synthetically-derived hetereocycle that targets the kinesin-5 or kinesin spindle protein Eg5. This protein plays an important role, inter alia, in the establishment of spindle bipolarity, a key facet of effective cell division.[12,13] As such, inhibitors of Eg5 are of considerable interest as potential therapeutic agents.[14,15]

In the period since our original studies on compound (+)-**1** legislation introduced by the Brazilian Government,[16] and designed to protect native flora and fauna, prevented the securing of further material from its natural source. Accordingly, the synthetic chemistry program detailed in the Supporting Information (SI) was undertaken and provided the (±)-, (+)- and (–)-forms of compound **1** each of which was assayed against the HL-60 (promyelocytic leukemia), HCT-116 (colon), OVCAR-8 (ovarian adenocarcinoma) and SF-295 (glyoblastoma) tumor cell-lines with doxorubicin (Dox) being used as the positive control. As revealed in Table 1, and consistent with our earlier studies[4] on the natural material, pterocarpan (+)-**1** was the most active against all of these tumor cell lines, with IC_{50} values varying between 0.20 to 3.61 μM, the highest activity being exerted on HL-60 (IC_{50} 0.20 μM). Interestingly, the levorotatory pterocarpan [(–)-**1**] was significantly less cytotoxic with the values for the racemate being more closely related to the cytotoxicity of enantiomer (+)-**1**. These results not only confirm the pivotal role of the absolute stereochemistry of the title pterocarpans on cytotoxicity but also highlight the potency of compound (+)-**1** by virtue of its similarities in activity in most of these assays to the clinically deployed anti-cancer agent doxorubicin (Dox).

Table 1. Cytotoxic activity (as determined via an MTT assay after 72 h) of (+)- , (–)- and (±)-2,3,9-trimethoxypterocarpan against selected tumor cell lines.[a]

Sample	Cancer Cell Line			
	HL-60	**HCT-116**	**OVCAR-8**	**SF-295**
	IC_{50} $\mu g\,mL^{-1}$ (μM values in brackets) ± SEM			
(+)-**1**	0.06 (0.20) ± 0.03	0.73 (2.42) ± 0.28	0.54 (1.79) ± 0.16	1.09 (3.61) ± 0.17
(–)-**1**	> 25 (82.78)	11.85 (38.54) ± 0.48	> 25 (82.78)	9.91 (32.81) ± 0.70
(±)-**1**	0.23 (0.76) ± 0.11	3.43 (11.36) ± 0.80	1.79 (5.93) ± 0.67	4.22 (13.97) ± 1.99
Dox	0.02 (0.04) ± 0.01	nd[b]	0.34 (0.62) ± 0.05	0.04 (0.08) ± 0.01

[a]Data are presented as IC_{50} [μg/mL (μM values in brackets)] values ± standard error of measurement (SEM) obtained by non-linear regression analysis for all cell lines from three independent experiments. Doxorubicin (Dox) was used as positive control; [b]Not determined.

The OVCAR-8 cell line represents a severe ovarian carcinoma that is resistant to a number of therapies and normally only detected after metastasis (viz. at stages II-IV). Normal treatments often involve chemotherapy using combinations of paclitaxel and carboplatin.[17] Given its morbidity and that, as revealed above, it is significantly affected by the pterocarpans we sought to analyze the effect of compounds (±)-**1** and (+)-**1** on this cell line in more detail. Specifically, the impacts of differing concentrations (1, 2 and 4 μM) of these compounds on OVCAR-8 proliferation over an interval of 98 h were studied using the xCELLigence system. The specified concentrations of compounds were selected as a result of outcomes of the initial studies described above. Paclitaxel or PTX (0.05 μM) was used as positive control. As revealed in Figure 2, those tumor cells treated with the enantiopure pterocarpan (+)-**1** caused a reduction of cellular growth in a dose-dependent manner. At the highest concentration of this pterocarpan (4 μM), the cellular growth profile was similar to that observed, particularly over the first few hours after treatment, when the same cell line was treated with PTX at a concentration of 0.05 μM. In striking contrast, treatment of OVCAR-8 with the corresponding racemate [viz. (±)-**1**] at any one of three

concentrations (viz. at 1, 2 or 4 μM) had no impact whatsoever, yielding growth curves closely resembling those observed for the untreated cells.

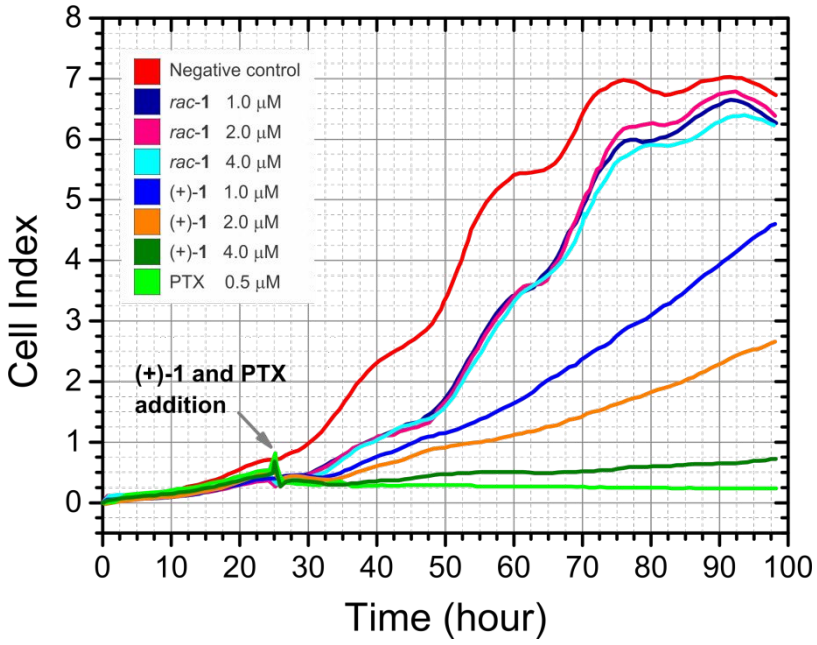

Figure 2. Growth curves observed for untreated OVCAR-8 cells and those treated with varying concentrations (1.0, 2.0 and 4.0 μM) of compounds (±)-**1**, (+)-**1** or paclitaxel (PTX – positive control at 0.5 μM). Data acquired using the xCELLigence system.

In order to delineate the anti-proliferative mechanism of action of compound (+)-**1** on the OVCAR-8 cell-line a flow cytometry analysis using propidium iodide as the fluorescent intercalating agent was performed. As revealed in Table 2, when these cells were treated with the racemate [*viz*. compound (±)-**1**] at concentrations of 5.0 or 10.0 μM for 24 h a significant increase of G2/M frequencies (42.06 ± 0.32 %) was observed albeit only at the higher dosage. In contrast, treatment of the cells with a 5.0 μM concentration of the enantiopure pterocarpan (+)-**1** exerted twice the effect (viz. 75.24 ± 5.57 % of the cells were arrested ones at the G2/M stage). At the higher concentration (10 μM) the percentage of arrested cells at G2/M stage was 79.13 ± 0.78 %. Our previous cell-cycle study[9] of the impact of treating MCF-7 breast cancer cells with naturally-derived (+)-**1** for 24 hours established that 32 ± 1.7% of them were arrested at the G2/M stage. So as to determine whether or not (+)-2,3,9-trimethoxypterocarpan [(+)-**1**] influences (potentiates) the

capacity of paclitaxel (PTX) to arrest the cell-cycle at the G2/M stage, the impacts of co-administering 2.5 μM and 0.05 μM solutions, respectively, of these compounds were studied. In the event, an increase in the percentage of cells arrested at the G2/M stage (78.62 ± 2.16 %) was observed when compared with the impacts of testing each of these compounds alone at the same concentrations [32.71 ± 0.56 % for (+)-**1** and 49.97 ± 1.34 % for PTX]. These results suggest that the two compounds act at different molecular targets.

Table 2. Flow cytometry analyses of the impacts of (±)-**1**, (+)-**1** and a (+)-**1**/PTX combination on the cell-cycle of OVCAR-8 cells after a 24 h incubation.

Sample	Concentration (μM)	DNA (%) ± S.D.		
		G_0/G_1	S	G_2/M
NC	-	67.06 ± 1.42	7.1 ± 0.86	25.78 ± 0.71
PTX	0.05	34.28 ± 1.62*	15.72 ± 0.30*	49.97 ± 1.34*
(±)-**1**	5.0	52.61 ± 0.15*	10.02 ± 0.39	37.16 ± 2.22
	10.0	46.72 ± 0.10*	10.93 ± 0.37*	42.06 ± 0.32*
(+)-**1**	2.5	58.16 ± 0.97	9.1 ± 0.40	32.71 ± 0.56
	5.0	15.83 ± 5.14*	8.76 ± 0.58	75.24 ± 5.57*
	10.0	10.84 ± 0.27*	9.92 ± 0.65	79.13 ± 0.78*
(+)-**1**/PTX	2.5/0.05	10.98 ± 0.08*	10.39 ± 2.06	78.62 ± 2.16*

Negative control (NC) was treated with the vehicle used for diluting the tested substance. Paclitaxel (PTX) at 0.05 μM was used as positive control. Experiments performed in independent triplicates with five thousand events per experiment. * $P < 0,05$, when compared with negative control through ANOVA followed by the application of Dunnett's test.

So as to establish whether the growth inhibition exerted by compound (+)-**1** arises through its inducing apoptosis and/or necrosis, treated OVCAR-8 cells were analyzed by fluorescence microscopy after dual acridine orange/ethidium bromide (AO/EB) staining and, thereby, the numbers of viable, apoptotic and necrotic cells were determined. As shown in Figure 3, after treatment of the cells with varying concentrations of (+)-2,3,9-trimethoxypterocarpan reductions in the number of viable ones occurred in a dose-dependent manner while there was also a corresponding increase of the number of apoptotic cells ($p < 0.01$) this being notably larger than

the number of necrotic cells being produced. Similar results were observed when the cells were treated with the positive controls doxorubicin (Dox) and paclitaxel (PTX).

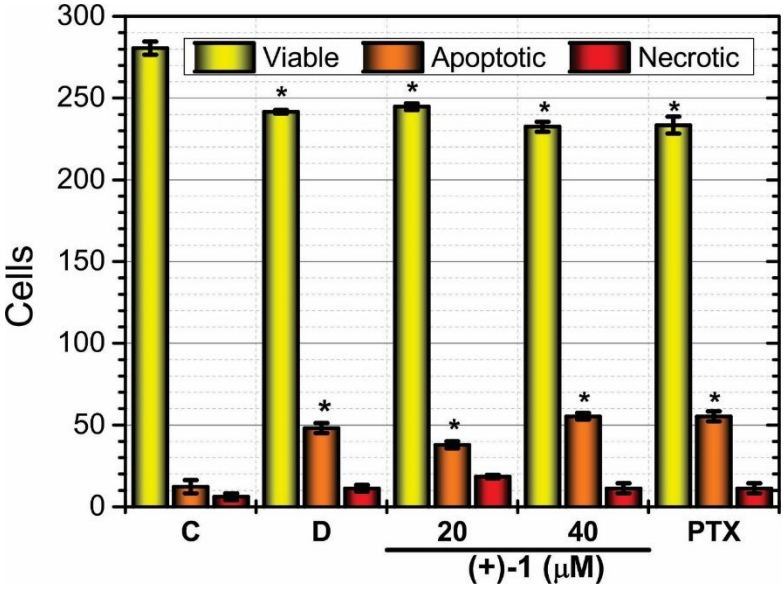

Figure 3. Effect of compound (+)-**1** on the viability of OVCAR-8 cells (viable cells – yellow bar; apoptotic cells – orange bar; necrotic cells – red bar) as determined by fluorescence microscopy after AO/EB staining and a 48 h incubation period. The data are presented as the mean values ± S.D. from three independent experiments performed in duplicate. The negative control (**C**) was treated with the same vehicle that diluted the tested substance (*viz*. 0.1% DMSO). Doxorubicin (**D**; 0.6 μM) and paclitaxel (**PTX**; 0.03 μM) served as the positive controls.* $p<0.05$ compared to the negative control as determined through ANOVA followed by the application of Dunnett's test.

Hematoxylin and eosin staining techniques were applied to both treated and untreated cells so as to gain insights into their morphologies. Specifically, after a 24 h incubation period, such an examination of the OVCAR-8 cells revealed drug-mediated changes. So, while the control (untreated) cells exhibited typical non-adherent, round morphology with vacuolization (Figure 4), those exposed to compound (+)-**1** (at concentrations of 20 and 40 μM) displayed chromatin condensation, a morphological hallmark of apoptosis. Paclitaxel (0.03 μM) showed the same behavior after treatment, including a reduction in cell volume, chromatin condensation and nuclear fragmentation (Figure 4).

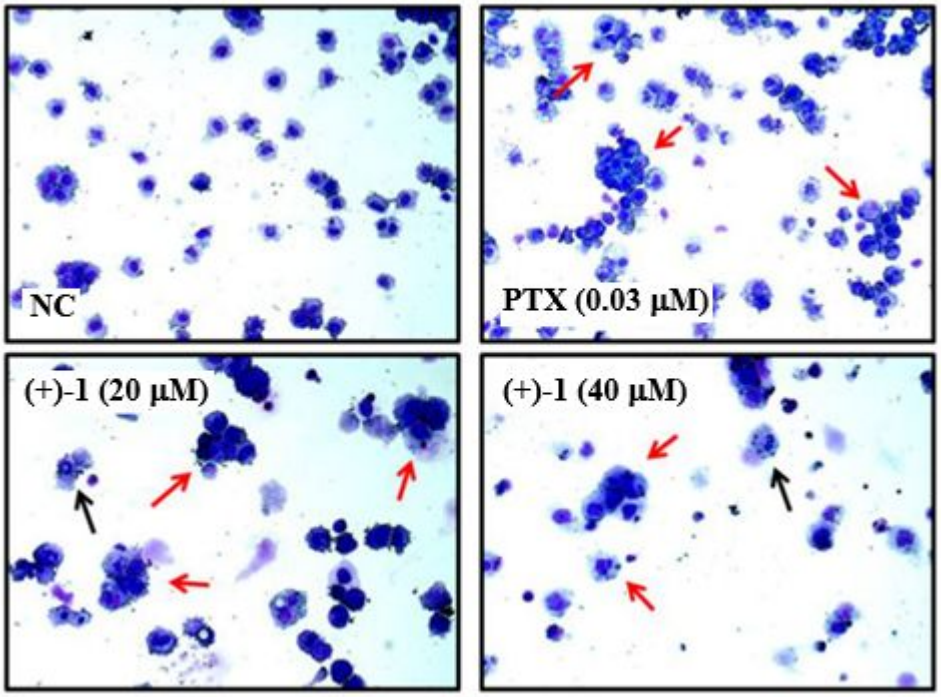

Figure 4. The effect of compound (+)-**1** (at 20 and 40 μM concentrations) on the morphology of OVCAR-8 cells. The cells were stained with hematoxylin and eosin then analyzed by optical microscopy after a 48 h incubation period. In the negative control (NC) experiment the cells were treated with the same vehicle (0.1% DMSO) used to dilute the test compound. Paclitaxel (PTX, at a concentration of 0.03 μM) served as the positive control. The black arrows show apoptotic bodies while the red ones highlight those (bodies) in which cell division has been arrested.

The foregoing results and our earlier ones[6,7,9] suggest that compound (+)-**1** and PTX have complementary modes of action with the former causing cell death through the triggering of apoptosis. As such and given both its potency and cytoselective properties, (+)-2,3,9-trimethoxypterocarpan warrants further investigation as a drug development candidate but to do so requires a more detailed understanding of its biological target and how it might interact with this. As noted above, various of our earlier studies[6,7,9] on the naturally-derived (+)-enantiomeric form of 2,3,9-trimethoxypterocarpan led us to conclude that its most likely receptor is the protein Eg5. Since a 1.8 Å resolution X-ray crystal structure of the Eg5 motor domain co-crystallized with MON has been reported[18] we sought to use these data for the purposes of establishing, through *in silico* studies, whether compound (+)-**1** has any capacity to dock in the allosteric pocket of Eg5 and, if so, to compute the energy of interaction of the resulting complex. In the event, on

undertaking the relevant molecular docking studies (see SI for details) these revealed that compound (+)-**1** seemed disposed toward binding with Eg5 (Figure 5) in the same region previously reported[11,19] for MON-Eg5 interaction. Through flexible ligand docking, the lowest energy associated to the best pose of potential inhibitor (+)-**1** inside the protein (when the latter was modeled in a fixed conformation) was −7.58 kcal/mol. This seemingly favored binding mode features the nesting of compound (+)-**1** between the distal Arg119 (in the main pocket) and Arg221 (in the minor pocket) residues, a interaction absent in the MON-Eg5 complex.[19] In this same pose compound (+)-**1** forms hydrophobic interactions, within the main cavity, with the Glu116, Gly117, Glu118, Trp127, Ala133, Ile136, Pro137, Tyr211, Leu214 and Glu215 residues while there is π-alkyl interaction of the benzopyran (chromane) ring of the pterocarpan with the Arg221 residue. Hydrogen bonding with the Arg119 residue also seems likely.

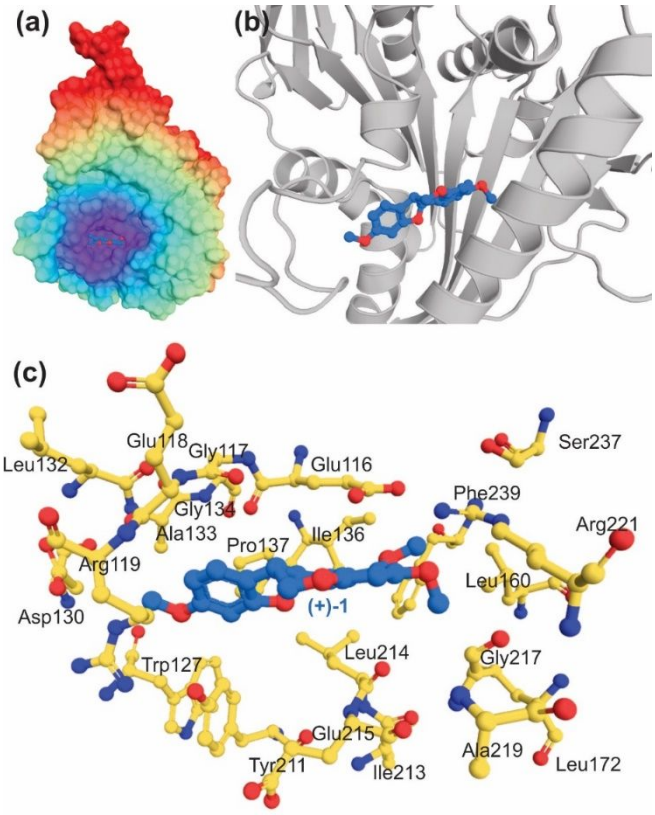

Figure 5. Molecular docking between Eg5 and compound (+)-**1**. (a) Eg5 binding site (blue) where (+)-**1** showed greatest stability. (b) The best conformation of (+)-**1** docked in a conformationally rigid form of the protein. (c) Most relevant amino-acid residues contributing to the stability of the (+)-**1**-Eg5 complex.

The molecular fragmentation with conjugated caps or MFCC technique[20-22] has been highlighted as a useful one for calculating, rather precisely, the interaction energies associated with protein-ligand complexes and so this was applied in the present setting. To such ends, an imaginary layer of radii r was identified, with each contributing value representing the shortest distance between the amino-acid of interest and the ligand and through a summation of these a binding pocket layer (BPL) was defined. A binding pocket of radius r, BP(r), was established as the set of amino-acid residues with at least one atom inside the corresponding BPL. Thereby, the total interaction energy, E(r), of the ligand complexed with Eg5 was determined as a function of r and calculated by summing the energies of all the interacting elements inside BP(r). The value of E(r) as a function of increasing values of BP(r), and wherein more and more amino-acid residues were considered, was then calculated. Figure 6 shows the resulting values for the interaction

energies of pterocarpan (+)-**1** and MON with Eg5 as a function of r (recorded in Å). The profiles of these were similar with the values for compound (+)-**1** being, almost invariably, lower (more negative) than the corresponding ones for MON. Both curves "stabilized" at an r value of ca. 10 Å with the interaction energies at this point being –219.09 kcal/mol for (+)-**1** and –216.10 kcal/mol for MON and thus very similar in magnitude. The most notable variation between the curves occurred when r was close to 5 Å and at which point the interaction energy continued to decrease for the pterocarpan but increased, over the 5 to 6 Å, range for MON.

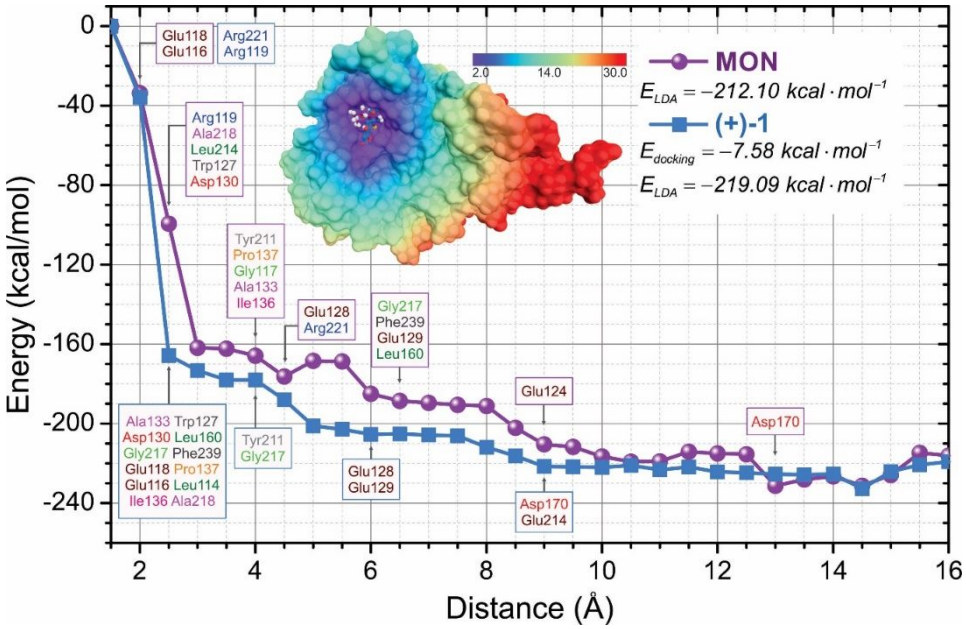

Figure 6. The total interaction energies of the (+)-**1**-Eg5 (blue squares) and MON-Eg5 (purple balls) complexes as a function of the binding pocket distance from the ligand and calculated using the MFCC method (key amino-acid residues involved in the binding interaction are shown). The inset shows the protein surface color map value based on proximity to the ligand and highlights the molecular pose of this in the binding pocket.

Parts (a) and (b) of Figure 7 show both the line diagrams and three-dimensional chemical structures of MON and compound (+)-**1**, respectively, as well as highlighting the various key and chemically similar substructures within them while the remaining parts (c and d) illustrate the best

fit of these compounds within Eg5 binding pocket. In another portrayal of the binding modes of these two ligands, Figure 8 serves to quantitate both the favorable (bars to the left) and unfavorable (bars to the right) interaction energies (in kcal/mol) between the associated substructures and the key amino-acid residues associated the binding region of Eg5. The region (boldface letters) and the atoms of the ligand which are closer to each residue at the binding site are specified at the end of these bars. For distances (r) shorter than 11.0 Å, the Arg221, Leu214, Glu116, Leu160, Arg119, Asp130, Trp127, Pro137, Ala133, Glu128, Ile136, Glu167, Ala218, Tyr211, Phe239, Glu129, Asp170, Glu124 and Gly117 residues of Eg5 contributed, as listed in descending order with respect to (+)-**1**, to the stabilizing interactions with both ligands. Within the same range, Gly217, also enhanced binding with (+)-**1** but had the opposite effect on MON binding. In descending order of effect, the protein residues contributing to the binding of MON were Arg119, Glu116, Leu214, Pro137, Glu167, Ala133, Glu118, Tyr211, Trp127, Glu128, Glu129, Glu124, Asp130, Ile136, Ala218, Arg221 and Phe239, a trend revealing that the most important difference in the binding of the two ligands involves Arg221 (Figure 8) since region iv of the pterocarpan (Figure 7b), *viz*. that involving the C2 methoxy group, is much closer to this residue as compared to the analogous region (i) (Figure 7a) of MON (1.8 *vs* 4.9 Å).

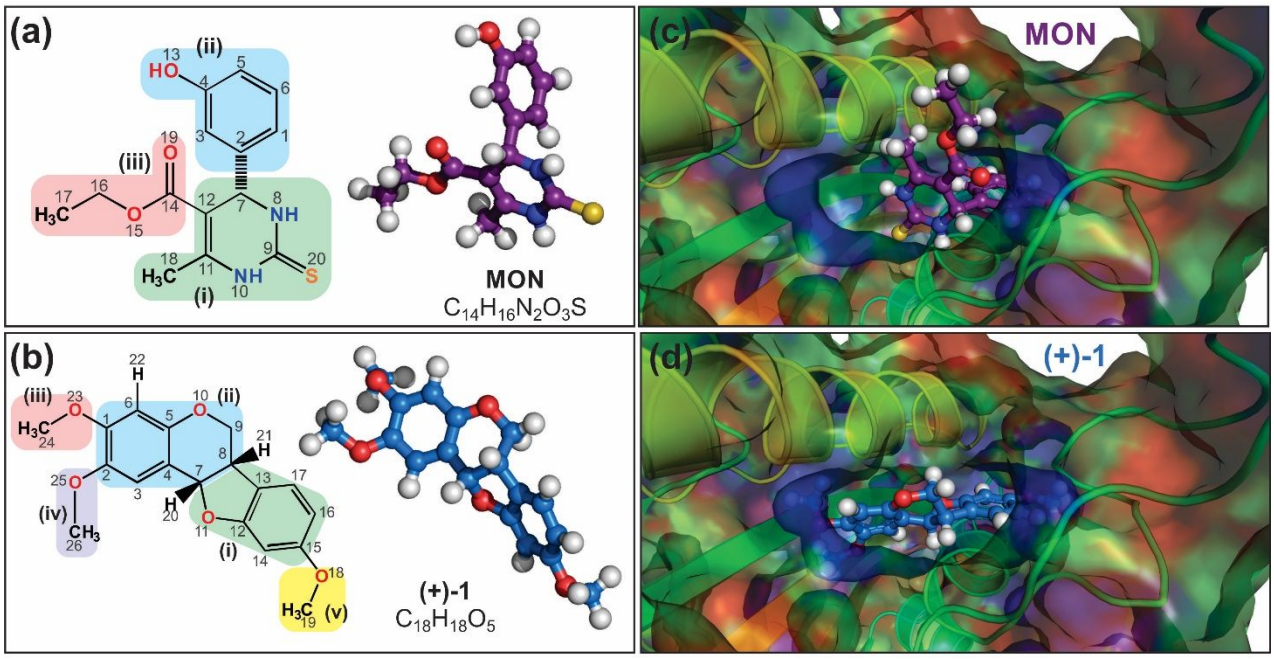

Figure 7. (a and b) The 2-D and 3-D chemical structures of MON and (+)-**1**, respectively [the colored highlights show key binding regions within MON and (+)-**1**]. (c and d) The Eg5 binding pocket containing MON (from co-crystallization data) and (+)-**1** (pose after docking), respectively.

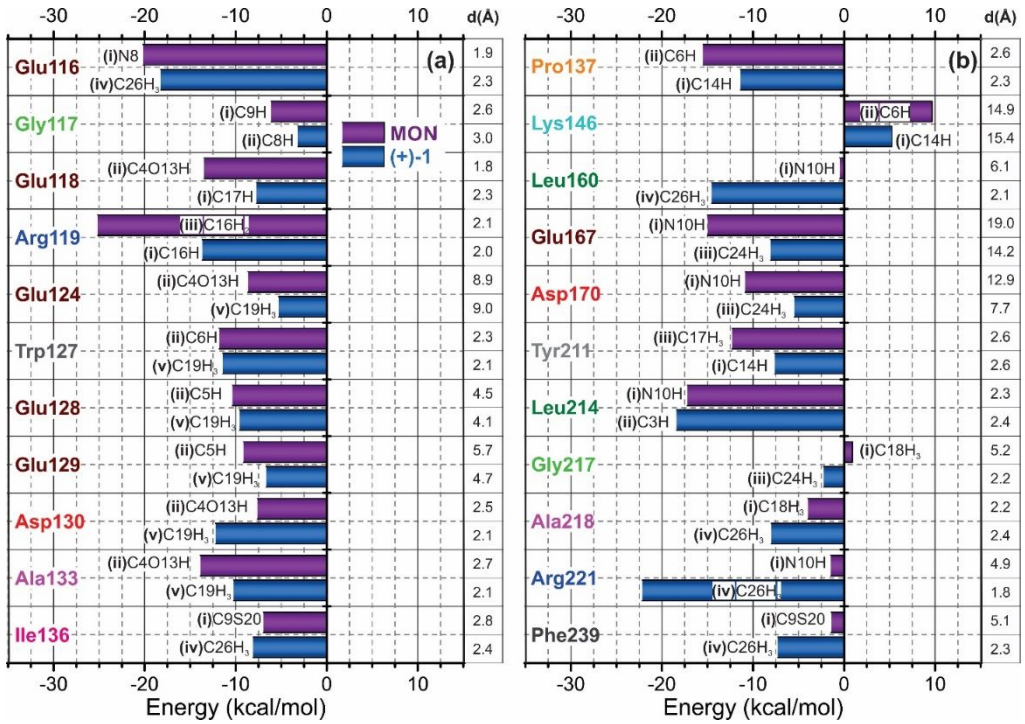

Figure 8. The key amino-acid residues of Eg5 interacting with MON (purple bars) and (+)-**1** (blue bars) and their respective energy contributions. Ligand atoms close to the relevant amino-acid residues of Eg5 are specified at the end of each bar.

The data shown in Figure 8 also reveals that Glu116 is the most important Eg5 residue involved in binding to both ligands (ca. 20 kcal/mol in both instances) and this is the result of hydrogen bonding between one of the O-C=O oxygens of Glu116 with the C26-bound hydrogen of the methoxy group located in region (iv) of the pterocarpan or through a region (i)-derived N-H···N bond in the case of MON and wherein the contact distance is just 1.9 Å (from the chain nitrogen of the amino-acid). Other perspectives taken on the binding of the two ligands (see Figures S3 and S4 in the SI for details) reveal that the benzofuran and benzopyran residues associated with compound (+)-**1** engage in alkyl-type interactions (10 kcal /mol) with Ala133 and Pro137 residues as well as a π-alkyl type interaction (*ca*. 11 kcal/mol) with Arg119 (Figures 7b, 8 and S4d). Interactions equivalent to these were also observed for MON and mainly because of the phenolic group associated with region (ii) of this compound (see Figures 7a, 8 and S3). The Leu214 and Ala218 residues were also important for stabilization of the binding of (+)-**1** because they participated in two alkyl interactions with the benzene ring present in region (i) of the pterocarpan structure (Figures 7b, 8, S4c and S4d), these being of about 19 and 9 kcal/mol in value, respectively. In an overall sense, then, ligand (+)-**1** would appear to engage in tighter binding to Eg5 than MON and this is the result of the presence of the methoxy groups in the former, especially that located in region (iii) (see Figure 7b).

The work reported here clearly reveals that (+)-2,3,9-trimethoxypterocarpan [(+)-**1**], but not its enantiomer, is a potent cytotoxic compound that most likely exerts these effects through binding to the MON allosteric binding site of the kinesin-type protein Eg5 (and does so more strongly than MON). The computational identification of the key binding features that stabilize the (+)-**1**/Eg5 complex should allow for the development of more potent analogues and these, together with the natural product itself, could provide a pathway for establishing therapies to treat, for example, refractory OVCAR-8-type solid tumors. Work directed toward such ends is now underway.

ASSOCIATED CONTENT

Supporting Information

The Supporting Information is available free-of-charge at https://pubs.acs.org/doi/10.1021/acsmedchemlett.XXXXX.

Synthetic scheme and associated commentary as well as full experimental details for the preparation of key compounds, crystallographic data, biological and theoretical protocols together with additional details of the docking of (+)-**1** and MON with Eg5.

AUTHOR INFORMATION

Corresponding Authors

Martin G. Banwell – Research School of Chemistry, Institute of Advanced Studies, The Australian National University, Canberra, ACT 2601, Australia and Institute for Advanced and Applied Chemical Synthesis, Jinan University, Guangzhou, 510632, China. Email: martin.banwell@anu.edu.au

Claudia do Ó. Pessoa – Department of Physiology and Pharmacology, Faculty of Medicine, Federal University of Ceará, Fortaleza, CE, 60430-275, Brazil. Email: cpessoa@ufc.br

Authors

Kaio Farias – Department of Physiology and Pharmacology, Faculty of Medicine, Federal University of Ceará, Fortaleza, CE, 60430-275, Brazil. Email: kaiomdf@yahoo.com.br

Roner F. da Costa – Department of Natural Sciences, Mathematics and Statistics, Federal Rural University of Semi-Arid Region - UFERSA, Mossoró - RN, Brazil. Email: ronerfc@gmail.com

Assuero S. Meira – Department of Physiology and Pharmacology, Faculty of Medicine, Federal University of Ceará, Fortaleza, CE, 60430-275, Brazil. Email: assueromeira@gmail.com

Jairo Diniz-Filho – Department of Physiology and Pharmacology, Faculty of Medicine, Federal University of Ceará, Fortaleza, CE, 60430-275, Brazil. Email: jdf@ufc.br

Eveline M. Bezerra – Department of Natural Sciences, Mathematics and Statistics, Federal Rural University of Semi-Arid - UFERSA, Mossoró - RN, Brazil. Email: evelinemb@gmail.com

Valder N. Freire – Department of Physics, Science Center, Federal University of Ceará, Fortaleza, CE, 60430-275, Brazil. Email: vnffreire@gmail.com

Prue Guest – Research School of Chemistry, Institute of Advanced Studies, The Australian National University, Canberra, ACT 2601, Australia. Email: prudence.guest@gmail.com

Maryam Nikahd – Research School of Chemistry, Institute of Advanced Studies, The Australian National University, Canberra, ACT 2601, Australia. Email: nikahd8513@yahoo.com

Xinghua Ma – Research School of Chemistry, Institute of Advanced Studies, The Australian National University, Canberra, ACT 2601, Australia. Email: hua@rsc.anu.edu.au>

Michael G. Gardiner – Research School of Chemistry, Institute of Advanced Studies, The Australian National University, Canberra, ACT 2601, Australia. Email: michael.gardiner@anu.edu.au

Manoel O. de Moraes – Department of Physiology and Pharmacology, Faculty of Medicine, Federal University of Ceará, Fortaleza, CE, 60430-275, Brazil. Email: odorico@ufc.br

Maria da C. F. de Oliveira – Department of Organic and Inorganic Chemistry, Science Center, Federal University of Ceará, Fortaleza, CE, 60430-275, Brazil. Email: mcfo@ufc.br

Complete contact information is available at: https://pubs.acs.org/10.1021/acsmedchemlett.XXXX

Author Contributions

The manuscript was written through contributions of all authors. All authors have given approval to the final version of the manuscript.

Notes

The authors declare no competing financial interests.

ACKNOWLEDGMENTS

This study was financed in part by the Coordenação de Aperfeiçoamento de Pessoal de Nível Superior - Brasil (CAPES) - Finance Code 001 - CAPES-Print Process nr. 88887.311918/2018-00; The authors are grateful to Conselho Nacional de Desenvolvimento Científico e Tecnológico (CNPq) for the financial support of the project (Process nr: 440755/2018-2 and 402329/2013-9) besides the research sponsorships of C. Pessoa (PQ-1B, Process nr: 303102/2013-6) and M. C. F. Oliveira (PQ-2, Process nr: 307667/2017-0). The support of the Australian Research Council and the Institute of Advanced Studies at the Australian National University is also gratefully acknowledged as is the Australian Government for the provision of a PhD scholarship (to PEG) and the Islamic Government of Iran for providing travel assistance (to MN).

REFERENCES

1. Rayan, A., Raiyn, J., Falah, M. Nature is the best source of anticancer drugs: Indexing natural products for their anticancer bioactivity. *PLoS*, **2017**, *12*(11), e0187925.

2. Paier, C. R. K., Maranhão, S. S'A., Carneiro, T. R., Lima, L. M., Rocha, D. D., da Silva Santos, R., Moraes de Faris, K., Odorico de Moraes-Filho, M., Pessoa, C. Natural products as new antimitotic compounds for anticancer drug development. *Clinics*, **2018**, *73* (suppl 1), e813s.

3. Al-Maharik, N. Isolation of naturally occurring novel isoflavonoids: an update. *Nat. Prod. Rep*. **2019**, *36*, 1156-1195.

4. Falcão, M. J. C., Brigido, Y., Pouliquem, M., Lima, M. A. S., Gramosa, N., Costa-Lotufo, L. V., Militão, G. C., Pessoa, C., Moraes, M.O., Silveira, E. R. Cytotoxic Flavonoids from *Platymiscium floribundum*. *J. Nat. Prod*. **2005**, *68*, 423-426.

5. Militão, G. C., Jimenez, P. C., Wilke, D. V., Pessoa, C., Falcão, M. J. C., Lima, M. A. S., Silveira, E. R., Moraes, M. O., Costa-Lotufo, L. V. (2005). Antimitotic Properties of Pterocarpans Isolated from *Platymiscium floribundum* on Sea Urchin Eggs. *Planta Medica*, **2005**, *71*(7), 683-685.

6. Militão, G. C., Dantas, I. N. F., Pessoa, C., Falcão, M. J. F., Silveira, E. R., Lima, M. A. S., Curi, R., Lima, T., Moraes, M. O., Costa-Lotufo, L. V. Induction of apoptosis by pterocarpans from *Platymiscium floribundum* in HL-60 human leukemia cells. *Life Sci.* **2006**, *78*(20), 2409-2417.

7. Militão, G. C., Bezerra, D. P., Pessoa, C., Moraes, M. O., Lima, M. A. S., Silveira, E. R. Costa-Lotufo, L. V. Comparative cytotoxicity of 2,3,9-trimethoxypterocarpan in leukemia cell lines (HL-60, Jurkat, Molt-4, and K562) and human peripheral blood mononuclear cells. *J. Nat. Med*. **2007**, *61*(2), 196-199.

8. Pueppke, S. G., VanEtten, H. D. Identification of three new pterocarpans (6a,11a-dihydro-6*H*-benzofuro[3,2-*c*][1]benzopyrans) from *Pisum sativum* infected with *Fusarium solani* f. sp. *pisi*. *J. Chem. Soc., Perkin Trans.* 1, **1975**, 946-8.

9. Militão, G. C., Prado, M. P., Pessoa, C., de Moraes, M. O., Silveira, E. R., Lima, M. A., Veloso, P. A. , Costa-Lotufo, L. V. Machado-Santelli, G. M. Pterocarpans induce tumor cell death through persistent mitotic arrest during prometaphase. *Biochimie*, **2014**, *104*, 147-155.

10. For related and recent work by others concerned with the biological evaluation of naturally-derived pterocarpans see Thuy, N. T. T., Lee, J.-E., Yoo, H. M., Cho, N. Antiproliferative Pterocarpans and Coumestans from Lespedeza bicolor. *J. Nat. Prod*. **2019**, *82*, 3025-3032.

11. Jiang, C., Chen, Y., Wang, X., You, Q. Docking studies on kinesin spindle protein inhibitors: an important cooperative ‘minor binding pocket’ which increases the binding affinity significantly. *J. Mol. Model*. **2007**, *13*, 987–992.

12. Chandrasekaran, G., Tátrai, P., Gergely, F. Hitting the brakes: targeting microtubule motors in cancer. *British J. Cancer* **2015**, *113*, 693–698.

13. Kim, C. D., Kim, E. D., Liu, L., Buckley, R. S., Parameswara, S., Kim, S., Wojcik, E. J. Small molecule allosteric uncoupling of microtubule deploymerase activity from motility in human Kinesin-5 during mitotic spindle assembly. *Sci. Rep*. **2019**, *9*, 19900.

14. For a recent commentary on the challenges and possibilities associated with establishing therapeutic agents based on Eg5 inhibition, see Zhang, W.; Zhai, L.; Lu, W.; Boohaker, R. J.; Padmalayam, I.; Li, Y.. Discovery of Novel Allosteric Eg5 Inhibitors Through Structure-Based Virtual Screening. *Chem. Biol. Drug Des.*, **2016**, *88*, 178-187.

15. Milic, B., Chakraborty A., Han, K., Bassik, M. C., Block, S. M. KIF15 nanomechanics and kinesin inhibitors, with implications for cancer chemotherapeutics. *PNAS*, **2018**, *115*, E4613-E4622.

16. Brancalion, P. H. S., Garcia, L. C., Loyola, R., Rodrigues, . R., Pillar, V. D., Lewinsohn, T. M. A critical analysis of the Native Vegetation Protection Law of Brazil (2012): updates and ongoing initiatives. *Natureza & Conservacão*, **2016**, *14*, 1-15.

17. Mitra, A. K., Davis, D. A., Tomar, S., Roy, L. , Gurler, H., Xie, J., Lantvit, D. D., Cardenas, H., Fang, F., Liu, Y., Loughran, E., Yang, J., Sharon, M. S., Emerson, R. E., Dahl, K. D. C., Barbolina, M. V., Nephew, K. P., Matei, D., Burdette, J. E. In vivo tumor growth of high-grade serous ovarian cancer cell lines. *Gynecologic Oncology*, **2015**, *138*(2), 372–377.

18. Maliga, Z., Xing, J., Cheung, H., Juszczak, L. J., Friedman, J. M. and Rosenfeld, S. S. A pathway of structural changes produced by monastrol binding to Eg5. *J. Biol. Chem*., **2006**, *281*, 7977–7982.

19. Kaan, H. Y. K., Ulaganathan, V., Hackney, D. D., Kozielski, F. An allosteric transition trapped in an intermediate state of a new kinesin-inhibitor complex. *Biochem. J*., **2010**, *425*(1), 55–61.

20. Zhang, D. W., Zhang, J. Z. H. Molecular fractionation with conjugate caps for full quantum mechanical calculation of protein–molecule interaction energy. *J. Chem. Phys*., **2003**, (119), 3599–3605;

21. Gordon, M. S., Fedorov, D. G., Pruitt, S. R., Slipchenko, L. V. Fragmentation Methods: A Route to Accurate Calculations on Large Systems. *Chem. Rev*. **2012**, *112*, 632-672.

22. Costa, R. F.; Feire, V. N., Cavada, B. S., Caetano, E. W. S.; Lima-Filho, J. L., Albuquerque, E.L. Explaining statin inhibition effectiveness of HMG-CoA reductase by quantum biochemistry computations. *Phys. Chem. Chem. Phys*. **2012**, *14*, 1389-1398.

ca. 150 Word Lay-Summary

Through synthetic chemistry studies the natural product (+)-2,3,9-trimethyoxypterocarpan, which, due to recently introduced environmental protection legislation, can no longer be extracted from its original source (a Brazilian tree), has been obtained. Testing of this compound against various cancer cell-lines, including a very aggressive one associated with breast cancer, reveals that it, but not its enantiomer, is very active while leaving healthy cells essentially untouched. The origins of this selectivity have been investigated and shown to involve the promotion of apoptosis (programed cell death) through interactions with Eg5, a protein involved in the assembly and maintenance of the mitotic spindle in dividing cells. The interaction of (+)-2,3,9-trimethyoxypterocarpan with Eg5 prevents the functioning of the latter and so slowing propagation of cancer cells. The detailed nature of this interaction has been revealed through high-level molecular modeling and thus offering the possibility of designing even more effective versions of the natural product.